



Removal of Cadmium in Aqueous Solution by Sulfidated Nanoscale Zero-Valent Iron

Weiyun Yang*, Ruolin Qin**, Rui Qin**, Linli Zhang** and Muqing Qiu***†

*Pharmaceutics and Materials Engineering School, Jinhua Polytechnic, Haitang West Street 888, Jinhua, 321007, P.R. China

**College of Life Science, Shaoxing University, Shaoxing, 312000, P.R. China

†Corresponding author: Muqing Qiu; qiumuqing@126.com

Nat. Env. & Poll. Tech.

Website: www.neptjournal.com

Received: 01-07-2019

Accepted: 30-08-2019

Key Words:

Cadmium removal;
Zero-valent iron;
Sulfidated nanoscale iron;
Aqueous solution

ABSTRACT

Due to mining, industrial wastewater discharge and agricultural fertilization and other human activities, heavy metal cadmium pollution in water bodies has become increasingly prominent. In this study, the sulfidated nanoscale zero-valent iron was prepared by the method of liquid-phase reduction. The removal behaviour of Cd(II) ion in aqueous solution and the effect of pH in solution on its removal rate were investigated. The synthesized materials before and after the adsorption reaction were characterized by scanning electron microscopy, X-ray diffraction and Zeta potential tester. The removal mechanism of Cd(II) ion in solution was explored in details. The results showed that the S-nZVI particles present a polymeric sheet. They contained Fe⁰, Fe₃O₄ and FeS. The removal rate of Cd(II) ion by the S-nZVI particles is higher than the nZVI particles. The reaction mechanism for S-nZVI particles to remove Cd(II) ion is that Cd(II) ion replaces Fe in FeS and then combines with S to form stable CdS compound. S has a significant effect on the oxidation process of iron.

INTRODUCTION

The heavy metal cadmium is a non-essential element of the human body. It mainly comes from the discharge of industrial wastewater such as mining, electroplating, batteries, smelting and dyes (Su et al. 2015). At present, the presence of heavy metal of cadmium can be detected in the environment (Lv et al. 2018). Compared with other heavy metals, cadmium has higher fluidity and is easily absorbed by plants. Additionally, it also can be enriched in the human body through the food chain, thus causing serious harm to human health (Qiu et al. 2018). Nowadays, the treatment techniques for removing cadmium from water mainly include adsorption, precipitation, ion exchange, membrane separation and so on (Zhang et al. 2014, Soleymanzadeh et al. 2015). Among these methods, the adsorption method mainly uses some chemical and biological adsorbents, such as activated carbon, hydrogel, carbon nanotubes, bagasse and so on. Precipitants commonly used in precipitation methods are sulphides, hydroxides and iron oxides (Gil-Díaz et al. 2017, Hu et al. 2017). These treatment techniques limit their large-scale applications due to cost or treatment efficiency issues. Therefore, there is an urgent need to develop more treatment methods for cadmium removal efficiency, low cost, and environmental friendliness.

Nano zero-valent iron (nZVI) is widely used in the pollution control of groundwater and soil heavy metals due to its high reactivity (Li et al. 2016, Zhu et al. 2019). The

nZVI particles have a unique core-shell structure in which the core is Fe(0) and the shell is FeOOH based iron oxide. In the processing of reaction with heavy metals, the nucleus acts as an effective electron donor to reduce the nZVI particles (Vaidotas et al. 2018). The shell provides adsorption points for the removal of heavy metals, and the core has a special complimentary effect with the shell (Li et al. 2017a). However, the removal efficiency of nZVI particles for heavy metal cadmium ion in solution close to its oxidation-reduction potential is low and unstable (Li et al. 2017b, Meghdad et al. 2019).

In recent years, many researchers have found that sulfidated nZVI particles can further increase its reactivity and selectivity, depending on the type and amount of sulfidated agent, the synthesis method and the target contaminant (Soleymanzadeh et al. 2015, Janja et al. 2018). The commonly used sulfidated agents for the preparation of sulfidated nZVI particles are sodium sulphide, sodium dithionite and sodium thiosulfate (Kong et al. 2016). In the study of the synthesis method, the synthesis according to the sulfidated agent is added before and after the formation of nZVI can be divided into a one-step method and a two-step method. Han & Yan (2016) studied the effects of different sulfidated agents and synthetic methods on the degradation of triethylene compounds. The results showed that the effect of the degradation rate of triethylene was independent of the

sulfidated agent and the synthesis method, but was related to the ratio of S/Fe. The S-nZVI particles were synthesized with a two-step process using Na_2S as a sulfidated agent and removed the $^{99}\text{TcO}_4^-$ ion in solution. The experimental results showed that $^{99}\text{TcO}_4^-$ was reduced to TcO_2 and fixed to the surface (Fan et al. 2013).

In this research, the main objective is 1) the S-nZVI particles were prepared by the method of liquid-phase reduction; 2) the adsorption of Cd(II) by the S-nZVI particles was tested; 3) The synthesized materials before and after the adsorption reaction were characterized by scanning electron microscopy, X-ray diffraction and Zeta potential tester; 4) The removal mechanism of Cd(II) ion in solution was explored.

MATERIALS AND METHODS

Preparation of S-nZVI

The S-nZVI was prepared by the method of liquid-phase reduction and a two-step method. 1 L 0.25 mol/L NaBH_4 solution was gradually added to a beaker containing 1 L 0.045 mol/L FeCl_3 solution. The solution was stirred by an electric stirring bar at the speed of 600 r/min, and the stirring operation was continued for 15 min after completion of the mixture reaction. The mixture was filtered through a Buchner funnel. The collected solid particles were rinsed 3 times with deionized water and then washed once with absolute ethanol. The nZVI particles were obtained. Ten g of nZVI particles

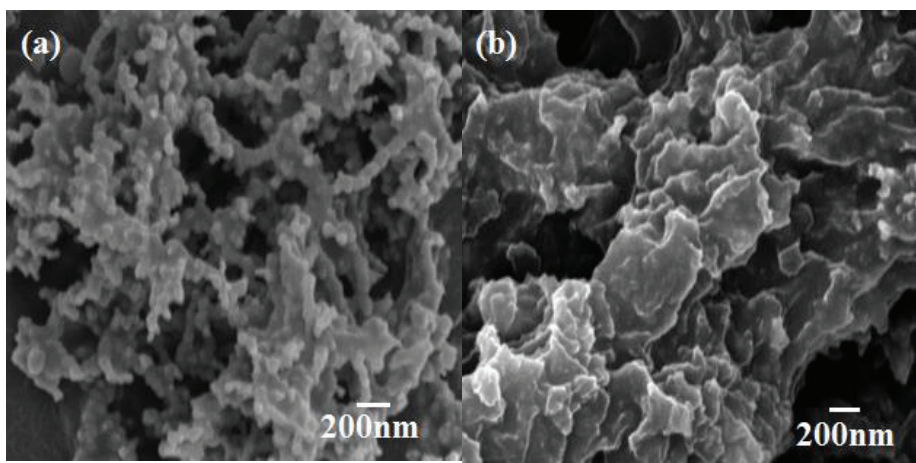


Fig. 1: SEM images of nZVI and S-nZVI [(a) nZVI particles and (b) S-nZVI particles].

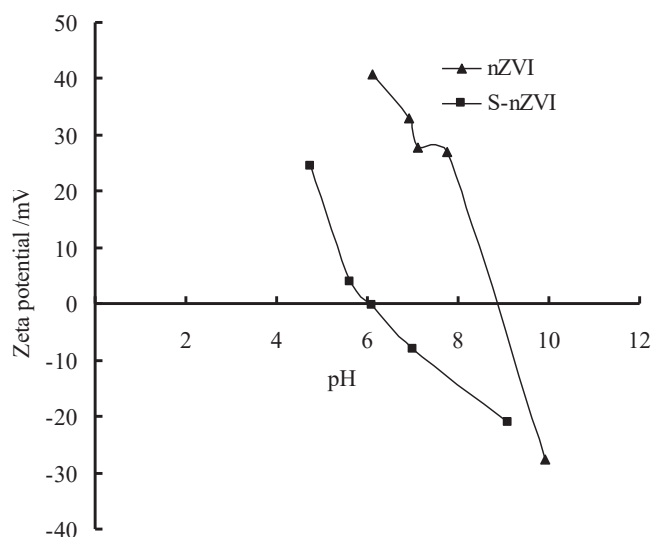


Fig. 2: The zeta potential of nZVI particles and S-nZVI particles as a function of pH.

were weighed into a 250 mL beaker containing 150 mL 215 g/L Na_2S solution and then shaken for 15 min at the speed of 600 r/min. Then, the S-nZVI particles were obtained for the experiment.

Characterization of S-nZVI

The morphology of S-nZVI particles was observed with SEM (JEOL 6500F, Japan). The XRD analysis was conducted in a D/Max-III A Powder X-ray Diffractometer (Rigaku Corp., Japan). The Zeta-potential was determined by Zeta potential tester (DT-1202, U.S.A.).

Adsorption Experiment

Adsorption experiments were conducted in a set of 250 mL Erlenmeyer flasks containing 0.1 g the S-nZVI and 100 mL of 200 mg/L Cd (II) ion solutions. The initial pH was adjusted to 4.0 with 1 mol/L HCl. The flasks were placed in a shaker at a constant temperature of 298 K and 200 rpm. The samples were filtered and analysed.

Analytical Methods

The concentration of cadmium ions was analysed by atomic absorption spectrophotometry. The amount of adsorbed Cd (II) ion q_t (mg/g) at different times, was calculated as follows:

$$Q = \frac{C_0 - C_t}{C_0} \times 100\% \quad \dots(1)$$

Where, C_0 and C_t (mg/L) are the initial and equilibrium

concentrations of Cd(II) ion in solution respectively. Q is the degradation rate of Cd(II) ion.

Statistical Analyses of Data

All the experiments were repeated in duplicate and the data of results were the mean and the standard deviation (SD). The value of the SD was calculated by Excel Software. All error estimates given in the text and error bars in figures are the standard deviation of means (mean \pm SD). All statistical significances were noted at $\alpha=0.05$ unless otherwise stated.

RESULTS AND DISCUSSION

Characterization of S-nZVI

The SEM images of the synthetic nZVI and S-nZVI are shown in Fig. 1. As can be seen from Fig. 1(a), the surface of synthetic nZVI particles exhibited a chain shape. After sulfidation, the surface of the S-nZVI particles exhibits a polymeric sheet structure (Fig. 2(b)).

Fig. 2 is a graph showing the zeta potential of nZVI particles and S-nZVI particles as a function of pH. It can be seen from Fig. 2 that as the pH increases, the zeta potential gradually changes from a positive value to a negative value. The zeta potential of nZVI particles and S-nZVI particles are 8.91 and 5.95.

The results of XRD in Fig. 3 showed that the synthetic nZVI particles have characteristic peaks at $2\theta=44.6^\circ$, 64.9° , 64.9° and 82.3° .

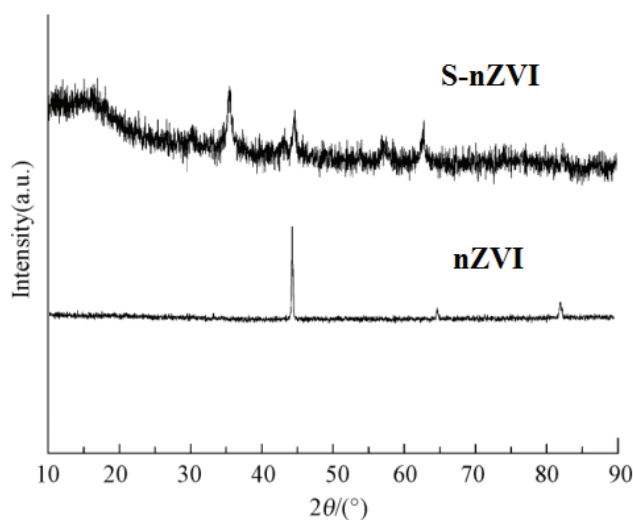


Fig. 3: XRD of nZVI particles and S-nZVI particles.

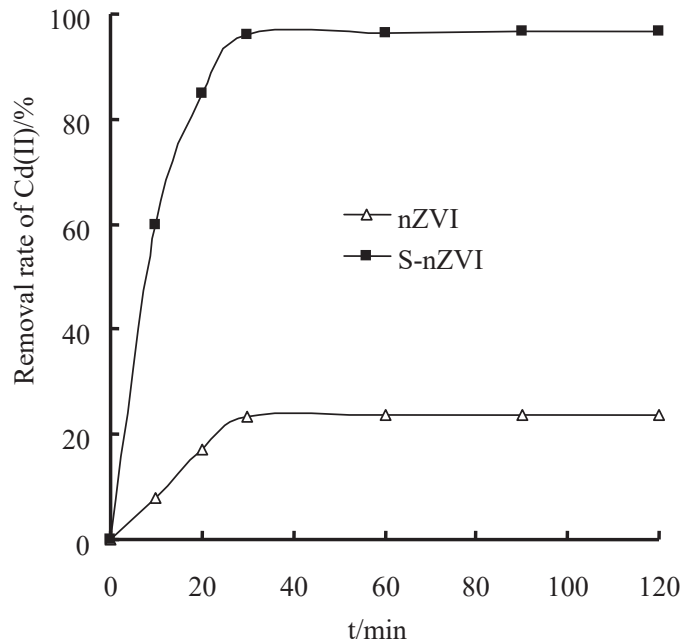


Fig. 4: Removal rate of Cd(II) ion by the nZVI particles and the S-nZVI particles.

This peak is the characteristic peak of $\alpha - Fe^0$. It also indicates that the synthetic nZVI particles are mainly present in the form of $\alpha - Fe^0$. There is no characteristic peak of iron oxide found in the synthetic nZVI particles. It may be the reason that the synthetic nZVI particles have low iron oxide content or a poor crystallinity and exist in an amorphous state (Sikder et al. 2014).

The synthetic S-nZVI particles detected a broad $\alpha - Fe^0$ peak at $2\theta=44.6^\circ$. It indicates that the crystallinity of $\alpha - Fe^0$

becomes low after the sulfidation treatment.

Besides, characteristic peaks of Fe_3O_4 and FeS were also detected. It indicates that the nZVI particles are loaded with S (Li et al. 2018).

Removal of Cadmium

Fig. 4 shows the removal rate of Cd(II) ion by the nZVI particles and the S-nZVI particles. As shown in Fig. 4, in the first 30 minutes, the removal rates of Cd(II) ion by the

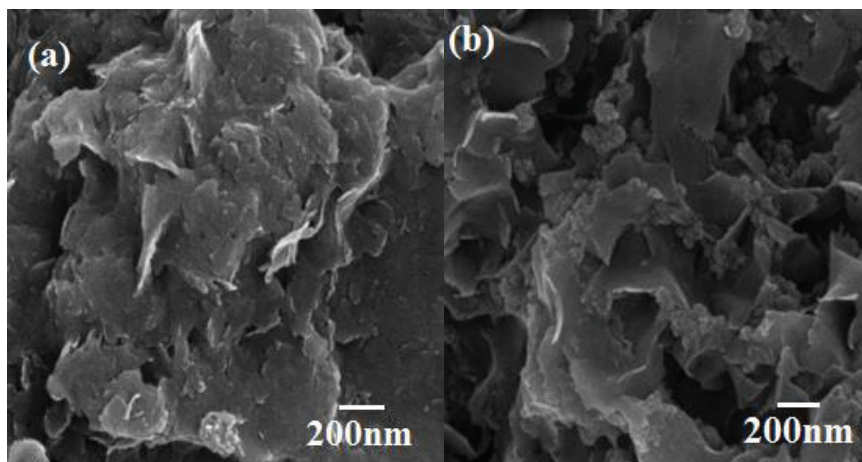


Fig. 5: SEM images of nZVI particles and S-nZVI particles after the reaction.

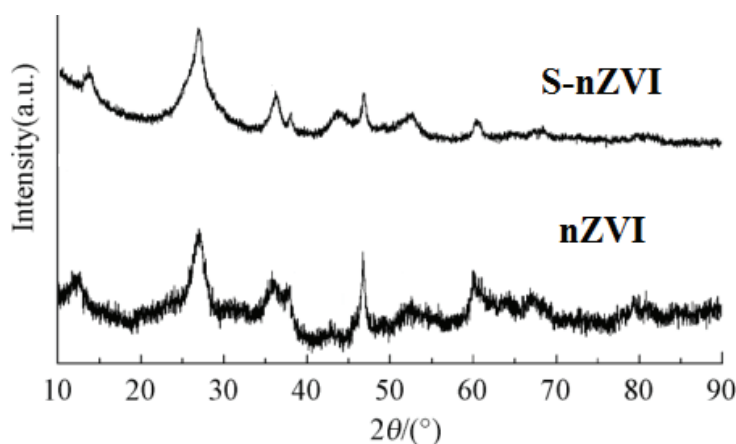


Fig. 6: XRD of nZVI particles and S-nZVI particles after the reaction.

nZVI particles and the S-nZVI particles are increasing. At 30 minutes, the removal rate of Cd(II) ion reached its maximum. Subsequently, the removal rate of Cd(II) ion increases very little. Additionally, the removal rate of Cd(II) ion by the S-nZVI particles is higher than the nZVI particles. The removal rate of Cd(II) ion by the S-nZVI particles reaches 96.1% at 30min.

Reaction Mechanism of Cadmium Removal

Fig. 5 is SEM images of the nZVI particles and S-nZVI particles after the reaction. As can be seen from the figure that the surface of the nZVI particles and S-nZVI particles is oxidized to a shape of a random sheet after reaction with Cd(II) ion in solution. The XRD of nZVI particles and S-nZVI particles after the reaction with Cd(II) ion is shown in Fig. 6.

It can be seen from Fig. 6 that there are strong $\gamma\text{-FeO(OH)}$ characteristic peaks in the nZVI particles and S-nZVI particles after the reaction with Cd(II) ion in solution. The FeS characteristic peak disappeared and a CdS characteristic peak was detected. This indicates that Cd(II) ion will react with Fe in FeS compound to generate CdS. Additionally, the weak S^0 characteristic peaks were also detected. This may be due to the action of FeS in the reaction and the residual O_2 in the solution (Crane et al. 2018, Holmes & Crundwell 2013 and Xia et al. 2010). After the reaction of nZVI with Cd(II) ion, the iron oxidation product in the material is mainly $\gamma\text{-FeO(OH)}$. For S-nZVI, the iron oxidation product in the material is mainly $\gamma\text{-FeO(OH)}$ and $\alpha\text{-Fe}_2\text{O}_3$. This indicates that S has a significant effect on the oxidation process of iron (Hardiljeet et al. 2011, Xue et al. 2018).

CONCLUSIONS

(1) The S-nZVI particles were prepared by the method

of liquid-phase reduction and a two-step method. The S-nZVI particles present a polymeric sheet. They contain Fe^0 , Fe_3O_4 and FeS.

- (2) The removal rate of Cd(II) ion by the S-nZVI particles is higher than the nZVI particles.
- (3) The reaction mechanism for S-nZVI particles to remove of Cd(II) ion is that Cd(II) ion replaces Fe in FeS and then combines with S to form stable CdS compound. S has a significant effect on the oxidation process of iron.

ACKNOWLEDGEMENTS

This study was financially supported by the Project of Science and Technology Plan in Zhejiang Province (LGF19C030001 and LGF20C030001) and the Project of Science and Technology Plan in Shaoxing City (2017B70058).

REFERENCES

- Crane, R.A. and Sapsford, D.J. 2018. Selective formation of copper nanoparticles from acid mine drainage using nanoscale zerovalent iron particles. *J. Hazard. Mater.*, 347: 252-265.
- Fan, D., Anitori, P.R., Tebo, B.M., Tratnyek, P.G., Pacheco, J.S.L., Kukkadapu, R.K., Mark, H., Engelhard, M., Bowden, E. and Libor, K. 2013. Reductive sequestration of pertechnetate ($^{99}\text{TcO}_4^-$) by nano zerovalent iron (nZVI) transformed by abiotic sulfide. *Environ. Sci. Technol.*, 47: 5302-5310.
- Gil-Díaz, M., Pinilla, P., Alonso, J. and Lobo, M.C. 2017. Viability of a nanoremediation process in single or multi-metal(loid) contaminated soils. *J. Hazard. Mater.*, 321: 812-819.
- Han, Y.L. and Yan, W.L. 2016. Dechlorination of trichloroethene by zero-valent iron nanoparticles: reactivity enhancement through sulfidation treatment. *Environ. Sci. Technol.*, 50: 12992-13001.
- Hardiljeet, K.B., Meera, J. and Denis, M.O. 2011. Kinetics and thermodynamics of cadmium ion removal by adsorption onto nano zerovalent iron particles. *J. Hazard. Mater.*, 186: 458-465.
- Holmes, P.R. and Crundwell, F.K. 2013. Polysulfides do not cause passivation: Result from the dissolution of pyrite and implications for other sulfide minerals. *Hydrometallurgy*, 139: 101-110.

- Hu, B.W., Chen, G.H., Jin, C.G., Hu, J., Huang, C.C., Sheng, J., Sheng, G.D., Ma, J.Y. and Huang, Y.Y. 2017. Macroscopic and spectroscopic studies of the enhanced scavenging of Cr(VI) and Se(VI) from water by titanate nanotube anchored nanoscale zero-valent iron. *J. Hazard. Mater.*, 336: 214-221.
- Janja, V., Primož, O., Radmila, M., Ana, M. and Ščančar, J. 2018. Investigation of the behaviour of zero-valent iron nanoparticles and their interactions with Cd²⁺ in wastewater by single particle ICP-MS. *Sci. Total Environ.*, 634: 1259-1268.
- Kong, X.K., Han, Z.T., Zhang, W., Song, L. and Li, H. 2016. Synthesis of zeolite-supported microscale zero-valent iron for the removal of Cr⁶⁺ and Cd²⁺ from aqueous solution. *J. Environ. Manage.*, 169: 84-90.
- Li, B., Yang, L., Wang, C.Q., Zhang, Q.P., Liu, Q.C. and Li, Y.D. 2017a. Adsorption of Cd(II) from aqueous solutions by rape straw biochar derived from different modification processes. *Chemosphere*, 175: 332-340.
- Li, J., Chen, C.L., Zhu, K.R. and Wang, X.K. 2016. Nanoscale zero-valent iron particles modified on reduced graphene oxides using a plasma technique for Cd(II) removal. *J. Taiwan Inst. Chem. Eng.*, 59: 389-394.
- Li, S.L., Wang, W., Liang, F. and Zhang, W.X. 2017b. Heavy metal removal using nanoscale zero-valent iron (nZVI): Theory and application. *J. Hazard. Mater.*, 322: 163-171.
- Li, Z.T., Wang, L., Meng, J., Liu, X.M., Xu, J.M., Wang, F. and Brookes, P. 2018. Zeolite-supported nanoscale zero-valent iron: New findings on simultaneous adsorption of Cd(II), Pb(II), and As(III) in aqueous solution and soil. *J. Hazard. Mater.*, 344: 1-11.
- Lv, D., Zhou, X.X., Zhou, J.S., Liu, Y.L., Li, Y.Z., Yang, K.L., Lou, Z.M., Shams, A.B., Wu, D.L. and Xu, X.H. 2018. Design and characterization of sulfide-modified nanoscale zerovalent iron for cadmium(II) removal from aqueous solutions. *Appl. Sur. Sci.*, 442: 114-123.
- Meghdad, P., Sajad, M., Mohsen, S., Wang, X.K. and Negin, F. 2019. A new composite of nano zero-valent iron encapsulated in carbon dots for oxidative removal of bio-refractory antibiotics from water. *J. Clean. Prod.*, 209: 1523-1532.
- Qiu, M.Q., Wang, M., Zhao, Q.Z., Hu, B.W. and Zhu, Y.L. 2018. XANES and EXAFS investigation of uranium incorporation on nZVI in the presence of phosphate. *Chemosphere*, 201: 764-771.
- Sikder, M.T., Tanaka, S., Saito, T. and Kurasaki, M. 2014. Application of zerovalent iron impregnated chitosan-cboxymethyl- β -cyclodextrin composite beads as arsenic sorbent. *J. Environ. Chem. Eng.*, 2: 370-376.
- Soleymanzadeh, M., Arshadi, M., Salvacion, J.W.L. and SalimiVahid, F. 2015. A new and effective nanobiocomposite for sequestration of Cd(II) ions: Nanoscale zerovalent iron supported on sineguelas seed waste. *Chem. Eng. Res. Design*, 93: 696-709.
- Su, Y.M., Adeyemi, S.A., Arturo, A.K., Huang, Y.X., Dai, C.M., Zhou, X.F. and Zhang, Y.L. 2015. Magnetic sulfide-modified nanoscale zerovalent iron (S-nZVI) for dissolved metal ion removal. *Water Res.*, 74: 47-57.
- Vaidotas, D., Saulius, V. and Vaidotas, V. 2018. Batch removal of Cd(II), Cu(II), Ni(II), and Pb(II) ions using stabilized zero-valent iron nanoparticles. *Energy Procedia*, 147: 214-219.
- Xia, J.L., Yang, Y., He, H., Zhao, X.J., Liang, C.L., Zheng, L., Ma, C.Y., Zhao, Y.D., Nie, Z.Y. and Qiu, G.Z. 2010. Surface analysis of sulfur speciation on pyrite bioleached by extreme thermophile *Acidianus manzaensis* using Raman and XANES spectroscopy. *Hydrometallurgy*, 100: 129-135.
- Xue, W.J., Huang, D.L., Zeng, G.M., Wan, J., Zhang, C., Xu, R., Cheng, M. and Deng, R. 2018. Nanoscale zero-valent iron coated with rhamnolipid as an effective stabilizer for immobilization of Cd and Pb in river sediments. *J. Hazard. Mater.*, 341: 381-389.
- Zhang, Y.L., Li, Y.T., Dai, C.M., Zhou, X.F. and Zhang, W.X. 2014. Sequestration of Cd(II) with nanoscale zero-valent iron (nZVI): Characterization and test in a two-stage system. *Chem. Eng. J.*, 244: 218-226.
- Zhu, L., Tong, L.H., Zhao, N., Li, J. and Lv, Y.Z. 2019. Coupling interaction between porous biochar and nano zero valent iron/nano α -hydroxyl iron oxide improves the remediation efficiency of cadmium in aqueous solution. *Chemosphere*, 219: 493-503.